Quantitative Phase Diagrams of Branching and Annihilating Random Walks

Léonie Canet,[1] Hugues Chaté,[2] and Bertrand Delamotte[1]

[1] *Laboratoire de Physique Théorique et Hautes Énergies, Universités Paris VI Pierre et Marie Curie, Paris VII Denis Diderot, 2 place Jussieu, 75251 Paris cedex 05, France*

[2] *CEA-Service de Physique de l'État Condensé, Centre d'Études de Saclay, 91191 Gif-sur-Yvette, France*

(Dated: February 2, 2008)

We demonstrate the full power of nonperturbative renormalisation group methods for nonequilibrium situations by calculating the *quantitative* phase diagrams of simple branching and annihilating random walks and checking these results against careful numerical simulations. Specifically, we show, for the $2A \to \varnothing$, $A \to 2A$ case, that an absorbing phase transition exists in dimensions $d = 1$ to 6, and argue that mean field theory is restored not in $d = 3$, as suggested by previous analyses, but only in the limit $d \to \infty$.

PACS numbers: 05.10.-a, 64.60.Ak, 64.60.Ht, 82.20.-w

The non-universal properties of continuous phase transitions, both at and out of thermal equilibrium, are much more difficult to determine than universal quantities such as scaling exponents. The latter are generally accessible, even for strongly coupled systems, through perturbative calculations near critical dimensions, since renormalisation group (RG) transformations can then bring them in the vicinity of fixed points corresponding to weakly-coupled regimes. On the other hand, non-universal properties, such as phase diagrams, depend on the whole RG flow, which must be controlled to keep track of all the microscopic information. Such calculations are thus genuinely non-perturbative. This is usually tempered by the fact that the mean-field (or one-loop) approximation seems to capture semi-quantitatively the relevant non-universal physics of most equilibrium systems. Hence the common wisdom that trying to account for fluctuations is needless since they are not expected to qualitatively alter phase diagrams. In this Letter, performing non-perturbative renormalization group (NPRG) calculations checked against numerical simulations, we show that this belief is drastically infirmed for a simple and widely studied nonequilibrium model, whose universal properties are otherwise well-understood.

We treat the case of branching and annihilating random walks (BARW) where particles of a single species A diffuse at rate D and undergo the reactions $A \xrightarrow{\sigma} 2A$, $2A \xrightarrow{\lambda} \varnothing$. Whereas mean-field rate equations predict that for any nonzero σ, the system always reaches an active steady state, early simulations [1, 2] in one and two space dimensions have revealed the existence of a continuous transition to the empty absorbing state, with scaling exponents characteristic of the directed percolation (DP) universality class [3]. Cardy and Täuber [4] confirmed, through one-loop RG calculations, that fluctuations can indeed induce, for any nonzero annihilation rate λ, a dynamical DP transition in dimensions $d \leq 2$. Their analysis also suggested that mean field theory is recovered for $d > 2$, implying in particular that a transition can no longer occur in $d = 3$, in agreement with numerical results by Takayasu and Tretyakov [1].

Below we determine the *quantitative* phase diagrams of BARW $A \xrightarrow{\sigma} 2A$, $2A \xrightarrow{\lambda} \varnothing$ in dimensions 1 to 6, from which it follows that the one-loop phase diagrams are qualitatively wrong above $d = 2$, although perturbative RG does lead to the correct universal critical exponents. Our approach uses and demonstrates the full power of the NPRG method, which allows to calculate —in addition to the universal DP-class properties— non-universal quantities even beyond critical dimensions and weak coupling regimes. All our results are confirmed, at the quantitative level, by numerical simulations carefully tailored to approach, in a controlled way, the continuous time limit where the analysis is performed. Specifically, we show that DP-class transitions occur at any nonzero σ/D in all dimensions from 1 to 6, but beyond a minimal threshold $(\lambda/D)_{\rm th}$ for $d \geq 3$. The transition line drifts with increasing dimension, and $(\lambda/D)_{\rm th}$ seems to grow linearly with d. This suggests that the transition occurs for all d and that the mean field picture is realized only in infinite dimension. Finally we show that the slope of the transition lines can be inferred from the master equation of a simple two-site model.

We first briefly review the field theoretical formulation of BARW, and the nonequilibrium implementation of NPRG methods. The stochastic dynamics of BARW is described by a master equation, which governs the time evolution of the configurational probability $P(\{n_i\}, t)$. For instance the contribution of the birth and death processes at site i reads:

$$\mathrm{d}P(n_i,t) = \sigma\,\mathrm{d}t\big[(n_i-1)P(n_i-1,t) - n_iP(n_i,t)\big] + \lambda\,\mathrm{d}t\big[(n_i+2)(n_i+1)P(n_i+2,t) - n_i(n_i-1)P(n_i,t)\big] \quad (1)$$

This master equation can be turned into a path integral representation in terms of two fields ϕ and $\bar{\phi}$ [5]. Following [4], the generating functional of the correlation

functions reads $\mathcal{Z}[\phi,\bar\phi] = \int \mathcal{D}\phi\,\mathcal{D}\bar\phi\, \exp(-S[\phi,\bar\phi])$ with

$$S[\phi,\bar\phi] = \int \mathrm{d}^d r\,\mathrm{d}t\,\big[\bar\phi(\partial_t - D\nabla^2)\phi - \sigma\phi\bar\phi + \sqrt{2\lambda\sigma}(\bar\phi\phi^2 - \phi\bar\phi^2) + \lambda\phi^2\bar\phi^2\big]\,. \quad (2)$$

This field theory can be then investigated using the NPRG method. This formalism — the effective average action method [6] — is a continuous implementation, on successive momentum shells, of Wilson's block-spin concept. It consists in building a sequence of running effective actions Γ_k in which only fluctuations with momenta larger than the running momentum scale k are averaged. At the scale $k=\Lambda$ (Λ^{-1} corresponding to the underlying lattice spacing), no fluctuation is yet taken into account and $\Gamma_{k=\Lambda}$ coincides with the microscopic action S. At $k=0$, all fluctuations are integrated out and $\Gamma_{k=0}$ encompasses the macroscopic properties of the system as it generates the one particle-irreducible correlation functions. $\Gamma_{k=0}$ is the analogue of the Gibbs free energy Γ at thermal equilibrium. Γ_k thus interpolates between the microscopic action and the effective action. The outcome of this procedure is twofold. First, it constitutes a RG method in the usual sense, in that the universal properties of critical phenomena can be derived from the behaviour of the flow in the vicinity of fixed points. On the other hand, since the NPRG flow can relate microscopic quantities to the large-scale behaviour of the system, this procedure embodies a calculation of the effective action associated with specific microscopic models. It thus enables to compute nonuniversal quantities, which depend on the microscopic definition of the system. In this sense it radically differs from perturbative RG which loses memory of the microscopic details. Moreover, the flow equation of Γ_k is nonperturbative, and as the approximations used do not rely on the smallness of a parameter, they are not confined to weak-coupling regimes or to the vicinity of critical dimensions.

We now briefly sketch the construction of the effective action Γ_k that only includes large momentum fluctuations, and give its nonequilibrium NPRG flow [7] (see [6, 8] for a detailed derivation at thermal equilibrium). The low and high momentum fluctuation modes are separated by a scale dependent mass-like term $\Delta S_k(\phi,\bar\phi) = \int_q \Phi(-q)\hat R_k(q)\Phi^T(q)$ where $\Phi = (\bar\phi,\phi)$, and $\hat R_k(q)$ is a symmetric matrix with zeros on its diagonal, and a cutoff function $R_k(q)$ off its diagonal. This cutoff acts as an effective mass $R_k(q)\sim k^2$ for $q\ll k$ that suppresses the propagation of the low momentum modes, while not altering the high momentum ones, $R_k(q)\to 0$ for $q\gg k$. In this work, we use $R_k(q) = (k^2-q^2)\theta(k^2-q^2)$ [9], which leads to simple analytical expressions ($\theta(x)$ denoting the step function). Γ_k is obtained by a Legendre transform of $\log\mathcal{Z}_k$, modified by an additional contribution $\Delta S_k(\psi,\bar\psi)$ [$\bar\psi$ and ψ being the functional derivatives of $\log\mathcal{Z}_k$ w.r.t. sources], in order to ensure that the proper limits are recovered at the scales $k=0$ and $k=\Lambda$. An exact RG equation for the flow of Γ_k is easily derived and underlies the nonequilibrium NPRG formalism [7]:

$$\partial_k\Gamma_k(\psi,\bar\psi) = \frac{1}{2}\mathrm{Tr}\left\{[\hat\Gamma_k^{(2)} + \hat R_k]^{-1}\partial_k\hat R_k\right\}, \quad (3)$$

where $\hat\Gamma_k^{(2)}$ is the field-dependent matrix of the second functional derivatives of Γ_k, and Tr stands for matrix trace over internal indices and integration over the internal momentum and frequency. Eq. (3) is a functional equation which obviously cannot be solved exactly. To handle it, one has to *truncate* Γ_k. We here implement a standard truncation consisting in the leading order of a time and space derivative expansion of Γ_k, which reads:

$$\Gamma_k(\psi,\bar\psi) = \int \mathrm{d}^d r\,\mathrm{d}t\,[Z_k\bar\psi(\partial_t - D_k\nabla^2)\psi + V_k(\psi,\bar\psi)]. \quad (4)$$

We emphasize that the full functional dependence of $V_k(\psi,\bar\psi)$ is dealt with and this truncation hence embodies an accurate description of the steady and uniform configurations of the system, as supported by all previous studies at thermal equilibrium. We refer to [7, 8, 10, 11] for detailed discussions of the approximation schemes. The flow equations for Z_k, D_k and $V_k(\psi,\bar\psi)$ are given in [7]. They allow us to determine the phase diagrams of BARW $A \xrightarrow{\sigma} 2A$, $2A \xrightarrow{\lambda} \varnothing$ in any dimension. For this, we numerically integrate the flow equations from an arbitrary initial ultra-violet scale $k=\Lambda$ where $\Gamma_{k=\Lambda}$ identifies with the microscopic action (2) for given λ, σ and D, and we determine the phase of the system (at the final scale $k=0$) ensuing from this initial condition. Figure 1 (lines) shows the resulting phase boundaries for $d=1$ to 6.

Before commenting on the phase diagrams, we present numerical results which fully confirm them. No existing simulations are available for a quantitative comparison. Worse, in $d=3$, no transition was found [1]. In these simulations the rates σ, λ, and D were parameterized by a single free variable, a drastic constraint likely to prevent them from reaching the absorbing state. Moreover, in [1], a strict occupation restriction was enforced ("fermionic" model), at odds with the analytical context. Here, we adapt the efficient models introduced recently in [12] to simulate arbitrary BARW processes without strict occupation restriction. We first notice that modifying the models of [12] to study $A \xrightarrow{\sigma} 2A$, $2A \xrightarrow{\lambda} \varnothing$ for $d\geq 3$ readily provides evidence of the existence of DP-class transitions (not shown). This does not allow, however, a quantitative comparison with our analytical results. Reaching this aim requires to resort to a time discretisation Δt of the master equation which reproduces as accurately as possible the continuous time evolution. A proper discretisation is achieved in the limit of Δt small enough to ensure that ΔP also remains infinitesimal so that the obtained critical rates remain invariant under rescaling

Δt. We proceed as follows. At each time step, all sites i undergo a parallel update. The on-site reactions are ruled by the three independent rates σ, D and λ: each of the n_i particles is tested for branching and for diffusion to a nearest-neighbor with respective probabilities $\sigma\Delta t$ and $D\Delta t$ for each neighbor. Simultaneously, each of the $n_i(n_i-1)/2$ possible pairs are candidates for annihilation with probability $2\lambda\Delta t$ following Eq. (1). The occupation number n_i is then updated according to the successful trials and the diffusion moves are implemented. We observe that the alteration of critical rates induced by changing Δt to $\Delta t/10$ generally does not exceed a few percent as long as the probabilities $\sigma\Delta t$, $2\lambda\Delta t$ and $D\Delta t$ remain smaller than typically 10^{-3}. In this limit, draws such that the number of annihilated particles would be larger than n_i are exceedingly rare (and rejected anyway). It is only in these rather inefficient-looking regimes that we can ensure to approach the continuous time limit. The code remains however powerful because only (the typically few remaining) non-empty sites are visited. The critical rates are determined by tracking the decay of the total population starting from fully-occupied initial conditions. The critical point is characterized by an algebraic decay with the DP exponent $\delta = \beta z/\nu$, separating saturation (supercritical regime) from (quasi-) exponential decay. To obtain the typical accuracy of 2% of the results presented in Fig. 1 (symbols), system sizes up to 2^{24} sites, and simulation times of up to 10^8 steps were necessary.

Still, the comparison between the analytical and numerical phase diagrams requires the prior calibration of the axes λ/D and σ/D. Indeed, as simulations implement a discrete lattice version of the master equation, the "numerical" rates differ from the analytical ones by a spatial continuum limit. We therefore introduce an overall offset parameter C which can be interpreted as the ratio Λ_0/Λ of the corresponding underlying microscopic scales —respectively lattice Λ_0 and ultra-violet Λ. The ratios λ/D and σ/D are therefore corrected with regards to their scaling dimensions by factors C^{2-d} and C^2 (see Eq. (2)). The unique offset parameter C is fixed by fitting the NPRG thresholds $C^{2-d}(\lambda/D)_{\rm th}(d)$ to the numerical ones. This produces a very accurate match (Fig. 2(a)). The resulting rescaled analytical full transition lines then also closely match their numerical counterparts on the range of rates considered in all dimensions from 1 to 6, as displayed in Fig 1. [We have checked that fitting other quantities to fix C only mildly changes its value, which does not spoiled the agreement between the numerical and analytical diagrams.]

We now comment on the phase diagrams. Their main feature is that the phase transition exists in all probed dimensions, thus qualitatively invalidating the one-loop picture. For $d \geq 3$, the transition curves are almost parallel straight lines, crossing the λ/D axis at a nonzero threshold value $(\lambda/D)_{\rm th}$. Up to $d = 6$, this threshold

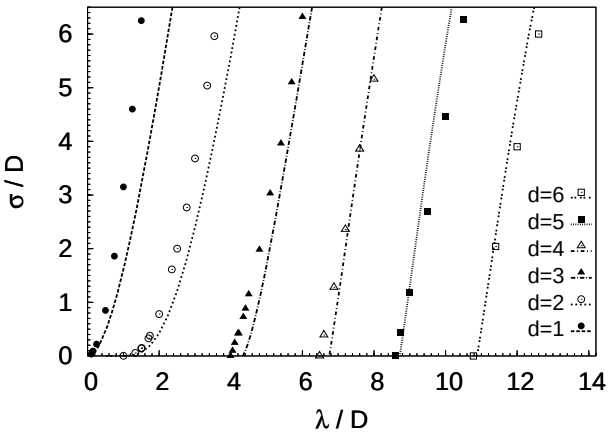

FIG. 1: Phase diagrams of BARW $A \xrightarrow{\sigma} 2A$, $2A \xrightarrow{\lambda} \varnothing$ in dimensions 1 to 6. Lines present NPRG results, rescaled as explained in the text. Symbols follow from numerical simulations. For each dimension, the active phase lies on the left of the transition line, the absorbing phase on the right.

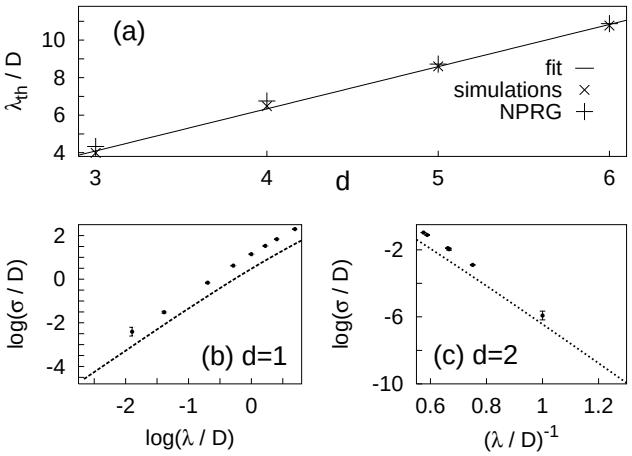

FIG. 2: (a): Evolution of the thresholds $(\lambda/D)_{\rm th}$ with the dimension; (b) and (c): log plots of the transition line in the vicinity of the origin in $d = 1$ and $d = 2$ with error bars.

grows linearly with d at a rate 2.248 ± 0.058, as extracted from a linear fit (see Fig 2(a)). Further theoretical calculations confirm that $(\lambda/D)_{\rm th}(d)$ is nearly linear at least up to $d = 10$. This suggests that $(\lambda/D)_{\rm th}$ becomes infinite in the limit $d \to \infty$, so that only the active phase remains in this limit. In other words, the mean field phase diagram seems to be recovered only at infinite dimension, that is neither in $d = 3$ (one-loop) nor in $d = 4$ (upper critical dimension). Below $d = 3$, the threshold vanishes. The approach of the transition curve to the origin is quadratic in $d = 1$, and exponential in $d = 2$ with a coefficient 11.86 ± 0.02 analytically, and 11.67 ± 0.15 numerically (Fig. 2(b) and (c)). This is in close agreement with the coefficient 4π predicted by perturbative RG (see [4] and [7]).

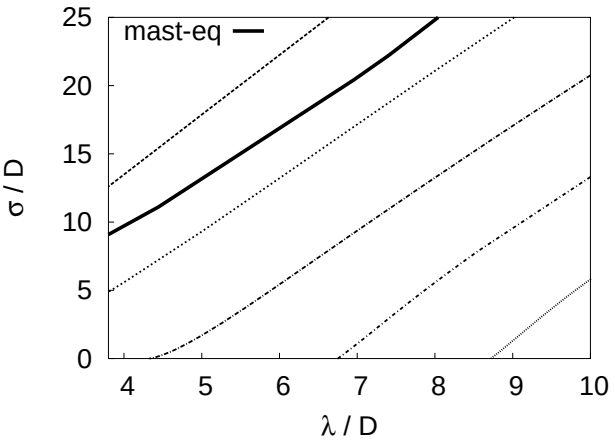

FIG. 3: Dashed lines: NPRG phase diagrams in $d = 1$ to $d = 5$ (from left to right); thick solid line: result from the two-site model.

We finally give a simple argument supporting our finding that in the weak diffusion regime the phase boundaries are almost straight lines. Indeed, an effective transition line can be estimated from the master equation itself in the limit of large σ/D and λ/D. If $D = 0$ exactly, sites are decoupled and the time evolution of each site can be considered independently. The evolution of the probability $P(n, t)$ at a given site is governed in this limit by the infinite set of coupled differential equations (1). One can readily prove from them that the unique stationary solution is $\{P(n = 0) = 1,\ P(n \geq 1) = 0\}$, which corresponds to the absorbing state. For $\sigma/\lambda \lesssim 10$, we have checked, by numerically integrating the master equations truncated to $n = 100$, that this state is the unique attractor reached at large times. (Including higher occupation number equations does not change this result.) Thus, for $D = 0$, the system always ends up in the absorbing phase at least up to $\sigma/\lambda \lesssim 10$ and probably for any finite σ/λ, with a relaxation time τ growing with σ/λ. We now argue that the absorbing state remains stable when a small diffusion is allowed. Qualitatively, we expect this to hold true as long as the diffusion time $(2dD)^{-1}$ ($2d$ standing for the number of neighbors), remains much larger than τ since then the particles on one site die before diffusing. To make this statement more quantitative, we consider the following model.

Near criticality, the system is very diluted, so we focus on an isolated single particle at site I, and model the rest of the lattice by a single, initially empty, neighboring site J. We numerically integrate a (30×30) truncation of the master equation for $P(\{n_I, n_J\}, t)$. Again, the system always reaches the absorbing phase, but we can assume that an active state can be sustained if the particle at site I manages to multiply and spread out to the neighbouring site before it dies out. We hence study the average occupation numbers $\bar{n}_I(t)$ and $\bar{n}_J(t)$. At given λ and σ, as long as $D = 0$, $\bar{n}_J(t) = 0$. When D is increased, $\bar{n}_J(t)$ starts to grow and reaches a maximum at $t = t_m$ before eventually vanishing. This leads us to set up the following criterion: the absorbing state is supposed to be destabilized if $\bar{n}_J(t_m)$ reaches one (while $\bar{n}_I(t_m) \geq 1$), which defines a critical diffusion rate D_c. Probing various σ/λ yields a nearly-straight transition line with approximately the observed constant slope (Fig. 3). This argument, as simple as it is, is by no means a rigorous proof, but provides further support to the existence of an absorbing state in the weak diffusion regime, in all finite dimensions.

In summary, we have provided a clear and coherent picture of the quantitative phase diagrams of BARW $A \xrightarrow{\sigma} 2A$, $2A \xrightarrow{\lambda} \varnothing$ for $d = 1$ to 6. We conclude that DP-class transitions probably exist in all space dimensions, and only occur beyond a minimum decay rate $(\lambda/D)_{\rm th}$ for $d > 2$. Note that it is the very existence of this threshold which dooms any perturbative approach. The close agreement between our simulations and our analytical results firmly roots the ability of the NPRG method to probe with great accuracy the nonuniversal behaviour of a specific model. This offers a promising means of investigation of other reaction-diffusion processes. Different types of BARW are obvious candidates [4], and future work will be devoted to explore the so-called PCPD ("pair-contact process with diffusion") $2A \to 3A$, $2A \to \varnothing$ [13].

B.D. wishes to thank G. Oshanin for fruitful discussions. The LPTHE is Unité Mixte du CNRS, UMR 7589.

[1] H. Takayasu and A. Y. Tretyakov, Phys. Rev. Lett. **68**, 3060 (1992).
[2] I. Jensen, Phys. Rev. E **47**, R1 (1993), Phys. Rev. Lett **70**, 1465 (1993), D. ben Avraham, F. Leyvraz, and S. Redner, Phys. Rev. E **50**, 1843 (1994).
[3] H. Hinrichsen, Adv. Phys. **49**, 815 (2000).
[4] J. L. Cardy and U. C. Täuber, Phys. Rev. Lett. **77**, 4780 (1996), J. Stat. Phys. **90**, 1 (1998).
[5] M. Doi, J. Phys. A **9**, 1479 (1976), L. Peliti, J. Phys. (Paris) **46**, 1469 (1984).
[6] N. Tetradis and C. Wetterich, Nucl. Phys. B [FS] **422**, 541 (1994).
[7] L. Canet, B. Delamotte, O. Deloubrière, and N. Wschebor, cond-mat/0309504.
[8] J. Berges, N. Tetradis, and C. Wetterich, Phys. Rep. **363**, 223 (2002).
[9] D. Litim, Phys. Rev. D **64**, 105007 (2001).
[10] T. R. Morris, Nucl. Phys. B **509**, 637 (1998).
[11] L. Canet, B. Delamotte, D. Mouhanna, and J. Vidal, Phys. Rev. D **67**, 065004 (2003).
[12] J. Kockelkoren and H. Chaté, Phys. Rev. Lett **90**, 125701/1 (2003).
[13] M. Henkel and H. Hinrichsen, cond-mat/0402433.